Letter

Precursors to Anderson localization in the Holstein model: Quantum and quantum-classical solutions

P. Mitrić,[1] V. Dobrosavljević,[2] and D. Tanasković[1]

[1]*Institute of Physics Belgrade, University of Belgrade, Pregrevica 118, 11080 Belgrade, Serbia*

[2]*Department of Physics and National High Magnetic Field Laboratory, Florida State University, Tallahassee, Florida 32306, USA*

(Received 26 December 2024; accepted 27 March 2025; published 7 April 2025; corrected 30 April 2025)

We calculate the frequency-dependent mobility of the Holstein polaron in one dimension near the adiabatic limit using the method based on dynamical quantum typicality, as well as the quantum-classical method. The agreement between fully quantum and quantum-classical solutions is very good. The most prominent feature is the appearance of a zero-frequency peak in the mobility, in addition to the displaced peak associated to the precursors of Anderson localization. The zero-frequency peak cannot be obtained within the phenomenological transient localization approach, which is often used in a semiquantitative description of charge transport in quasi-one-dimensional organic semiconductors.

DOI: 10.1103/PhysRevB.111.L161105

Introduction. Charge mobility is a key quantity which determines the optoelectronic properties of molecular organic semiconductors [1–3]. Weak van der Waals forces between the organic molecules lead to strong lattice thermal fluctuations and the charge transport in pure samples near room temperature is dominated by electron-phonon scattering. It is common to distinguish between the local electron-phonon interaction and its nonlocal part, which are often modeled by the Holstein and Peierls Hamiltonian, respectively. However, in many cases the electron-phonon scattering is too strong to be treated by perturbative methods [4], the charge transport is in between the band and the hopping limit [5], and a reliable quantum calculation of the dc mobility is lacking, even within these two simplified models. The real-frequency calculations are often restricted to lattices that are not sufficiently large [6,7], while the effectiveness of the imaginary-axis quantum Monte Carlo (QMC) calculations [8] is limited by the ill-defined analytical continuation [9], since a small difference in the imaginary-time current-current correlation function can correspond to a substantial difference in conductivity [10–12].

An important insight into the charge transport in quasi-one-dimensional organic semiconductors is obtained by the phenomenological transient localization (TL) theory [4,13]. It starts from the observation that on short timescales, much smaller than the period of lattice oscillation $2\pi/\omega_0$, the ion displacements can be considered as *almost static* and randomly distributed (with appropriate probability distribution). Hence, on these timescales, the charge transport can be described by the physics of an electron moving thorough the statically disordered environment. In a model of *fully static* disorder, i.e., in the Anderson model (AM), the electron wave functions would be localized in low dimensions. However, the phonons are a source of dynamical disorder, causing the inelastic scattering which breaks the localization at longer timescales. In the TL approach, which is not restricted to a particular model, the inelastic scattering is accounted in a relaxation time approximation through the phenomenological parameter $\tau_{\text{in}} \sim 1/\omega_0$ which, at long times, modifies the current-current correlation function corresponding to the AM, $C_{jj}^{\text{TL}}(t) = C_{jj}^{\text{AM}}(t)e^{-t/\tau_{\text{in}}}$, leading to nonzero dc mobility. The frequency-dependent mobility $\mu(\omega)$ features a so-called displaced Drude peak (DDP) [7], which is here a signature of precursors to the Anderson localization. Its appearance is, however, a more general phenomenon. DDP is observed in different physical systems, including some bad metals, and its origin is a subject of several recent studies [14–17].

Another popular approach to charge dynamics is given by the quantum-classical (QC) methods [18–20]. Here, the electron part of the Hamiltonian is treated quantum mechanically, whereas the lattice vibrations are treated classically. The backaction of the electron to lattice vibrations is usually included through the Ehrenfest equations. In this case, the total energy of the system is conserved, but the electron energy increases with the propagation time. At large times, the electron energy is not distributed according to the Boltzmann statistics at temperature T, but instead follows the distribution corresponding to infinite temperature. This feature has led to the conclusion that the QC method gives a divergent diffusion constant $D(t)$ at $t \to \infty$, implying that it cannot be used to calculate the dc mobility [4,13]. However, a very recent work [21] on the one-dimensional (1D) Peierls model for the parameter models corresponding to rubrene finds that $D(t)$ features an upturn at $t \approx 1/\omega_0$, but reaches a plateau for $t \sim 2\pi/\omega_0$. The upturn in $D(t)$ corresponds to a zero-frequency peak in the frequency-dependent mobility $\mu(\omega)$ of width ω_0, which is absent in the TL solution. Furthermore, it was shown that a similar result for $D(t)$ can be obtained within the newly developed mapping approach to surface hopping [21,22] which conserves the electron energy, giving important support to the Ehrenfest dynamics result. Still, there are important questions that have remained open. In particular, how applicable is the QC approximation? Will the zero-frequency peak appear also in the fully quantum solution? Does the answer depend on a specific model and the parameter regime?

To answer these questions, in this Letter we focus on the 1D Holstein model, where due to recent methodological advances, we can find a fully quantum solution representative of the thermodynamic limit, at least in certain parameter regimes. Specifically, we will use the method based on dynamical quantum typicality (QT) [23] which is complemented by the publicly available solutions of the hierarchical equations of motion (HEOM) [11,24,25]. We find very good agreement with the numerically cheaper QC calculations, both featuring nonmonotonous diffusion $D(t)$ with a plateau at large times. Both the fully quantum and QC solution feature a zero-frequency peak in $\mu(\omega)$, apart from the finite-frequency DDP which appears as a precursor to the Anderson localization at a short timescale. Our results, when combined with those for the Peierls model [12,21], indicate that the zero-frequency peak in mobility appears both in the models with local and nonlocal electron-phonon coupling.

Model and methods. The 1D Holstein model is given by the Hamiltonian

$$H = -t_0 \sum_i (c_i^\dagger c_{i+1} + \text{H.c.}) - g \sum_i n_i (a_i^\dagger + a_i) + \omega_0 \sum_i a_i^\dagger a_i. \quad (1)$$

Here, t_0 is the hopping parameter, $c_i^\dagger$ ($a_i^\dagger$) is the electron (phonon) creation operator, $n_i = c_i^\dagger c_i$, and we assume a single electron in the band as appropriate for low doped semiconductors. The electron-phonon coupling constant is denoted by g, the phonon frequency by ω_0, and we also introduce a convenient dimensionless quantity $\lambda = g^2/(2\omega_0 t_0)$. We set t_0, $\hbar$, k_B, e, and the lattice constant to one. Within the Kubo linear-response formalism [26–28], the time-dependent diffusion constant, $D(t) = \int_0^t dt' \,\mathrm{Re}\, C_{jj}(t')$, and the frequency-dependent mobility,

$$\mu(\omega) = \frac{2\tanh\left(\frac{\beta\omega}{2}\right)}{\omega} \int_0^\infty dt \cos(\omega t) \mathrm{Re}\, C_{jj}(t), \quad (2)$$

are obtained from the current-current correlation function $C_{jj}(t) = \langle j(t) j(0) \rangle$, where $j = i t_0 \sum_i (c_{i+1}^\dagger c_i - c_i^\dagger c_{i+1})$. The dc mobility is given by the Einstein relation $\mu_{\mathrm{dc}} = D(\infty)/T$.

We solve the Hamiltonian given by Eq. (1) by the methods which, in certain parameter regimes, give a numerically exact result for $C_{jj}(t)$ representative of the thermodynamic limit. The QT method [29,30] is presented in detail in Ref. [23]. Its application is mostly restricted by the computer memory since the Hilbert space grows rapidly with the total number of phonons and lattice sites that we take into account. We use it for intermediate and strong coupling, where one can eliminate the finite-size effects within available memory. For the solution at high temperature and for weak coupling, we use the HEOM results from the literature [24,25]. At low temperature we need a much longer chain, but for a weak interaction we can calculate the mobility within the dynamical mean-field theory (DMFT) [31]. In Ref. [32] we showed that, rather surprisingly, the DMFT gives nearly exact single-particle properties within the Holstein model, in an arbitrary number of dimensions and the corresponding exact self-energy is nearly local. The bubble term for conductivity then almost coincides in the HEOM and DMFT solutions [11]. Furthermore, we showed that the vertex corrections to conductivity in the Holstein model vanish in the weak-coupling limit [11]. That is why the DMFT solution for conductivity is almost exact in the weak-coupling limit.

In the QC solution the electron dynamics is obtained from a solution of the Schrödinger equation, while the ion dynamics is treated classically [18–20]. The electron Hamiltonian is given by

$$H^{\mathrm{el}} = -t_0 \sum_i (c_i^\dagger c_{i+1} + \text{H.c.}) - g\sqrt{2\omega_0} \sum_i x_i c_i^\dagger c_i, \quad (3)$$

where the displacement operator $x_i = (1/\sqrt{2\omega_0})(a_i^\dagger + a_i)$ is considered as a classical variable. The ion dynamics $x(t)$ is treated both within the classical path approximation (CPA) and the mean-field Ehrenfest method [20,21]. In CPA, the ions perform harmonic oscillations, $x_i(t) = x_i(0)\cos(\omega_0 t) + [\dot{x}_i(0)/\omega_0]\sin(\omega_0 t)$. Hence, in this case the ion dynamics is completely determined by the initial ion displacements and velocities. As we show in Supplemental Material (SM) Sec. I [33] (see also Refs. [34–39] therein), $x_i(0)$ and $\dot{x}_i(0)$ should be taken from the Gaussian distributions with the variance $\langle x_i^2(0) \rangle = \frac{1}{2\omega_0} \coth(\beta\omega_0/2)$ and $\langle \dot{x}_i^2(0) \rangle = \frac{\omega_0}{2} \coth(\beta\omega_0/2)$, respectively. In the mean-field Ehrenfest method the ion dynamics is modified by the presence of an electron by the backaction term $-\partial/\partial x_i \langle \langle \psi_n(t) | H^{\mathrm{el}} | \psi_n(t) \rangle \rangle$, where the outer angle bracket denotes averaging over the Boltzmann factor. The initial electron wave functions $\psi_n(0)$ correspond to the eigenstates of H^{el} with energy E_n obtained for random ion displacements and velocities, $H^{\mathrm{el}}(0)|\psi_n(0)\rangle = E_n |\psi_n(0)\rangle$. Then we use the fourth-order Runge-Kutta method for CPA or the second-order Verlet method for Ehrenfest dynamics, using a sufficiently small time step Δt, to calculate $\psi_n(t)$ from the time-dependent Schrödinger equation $i\frac{\partial}{\partial t}|\psi_n(t)\rangle = H^{\mathrm{el}}(t)|\psi_n(t)\rangle$. The current-current correlation function is then given by

$$C_{jj}(t) = \frac{1}{Z} \sum_{n,m} e^{-\beta E_n} \langle \psi_n(t) | j | \psi_m(t) \rangle \langle \psi_m | j | \psi_n \rangle, \quad (4)$$

which needs to be averaged over many realizations of the initial ion positions and velocities. The QC equations are described in more detail in SM Sec. I [33].

Results. We will present the results for $\omega_0 = 1/3$ at intermediate ($\lambda = 0.5$) and weak ($\lambda = 1/8$) electron-phonon coupling, and the results for $\omega_0 = 0.1$ at $\lambda = 0.45$ and 1.25.

The results for $\omega_0 = 1/3$, $\lambda = 0.5$ ($g = 0.577$), and $T = 1$ are shown in Fig. 1. We start our analysis from the two well-known limits. The DMFT solution [31,32] neglects the vertex corrections to conductivity. In this case the current-current correlation function $C_{\mathrm{jj}}^{\mathrm{DMFT}}(t)$ exponentially goes to zero [Fig. 1(a)] and the frequency-dependent mobility $\mu(\omega)$ assumes a Lorentzian shape [Fig. 1(b)]. Since the self-energy in the Holstein model is almost local [32], the DMFT solution practically coincides with the full quantum solution in the bubble approximation [11]. In the static case, when the ion vibrations are frozen at their randomly chosen $t = 0$ positions, we end up with the AM solution. In this case, $C_{jj}^{\mathrm{AM}}(t)$ changes sign and then, following a power law $\propto 1/t^2$, goes to zero, such that the dc mobility $\mu_{\mathrm{dc}} = \int_0^\infty C_{jj}^{\mathrm{AM}}(t) = 0$.

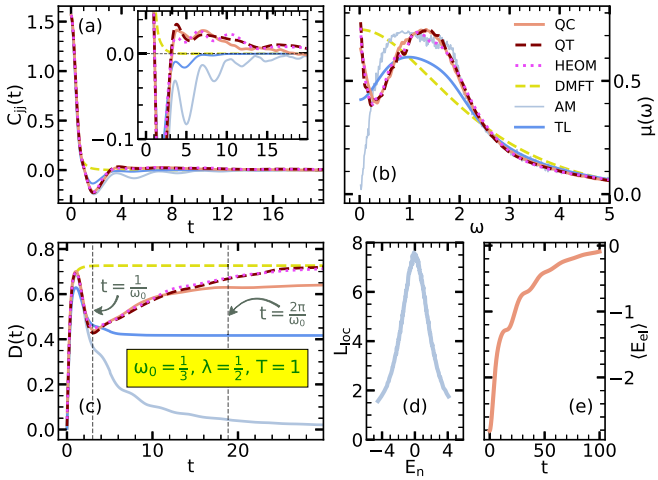

FIG. 1. Comparison between different methods of the (a) current-current correlation function, (b) frequency-dependent mobility, (c) time-dependent diffusion constant, (d) localization length, and (e) ensemble-averaged electron kinetic energy for intermediate electron-phonon coupling.

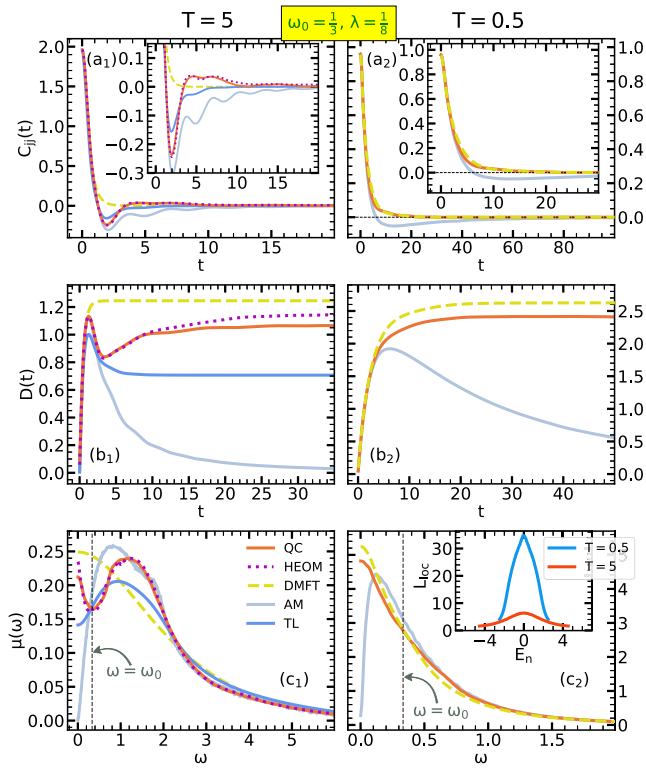

FIG. 2. (a) Current-current correlation function, (b) time-dependent diffusion constant, and (c) frequency-dependent mobility for weak electron-phonon coupling at high (left column) and low temperature (right column).

The qualitative difference which brings the full solution of the Holstein model is best understood by looking at the time-dependent diffusion constant $D(t)$ [Fig. 1(c)]. After the ballistic regime where $D(t)$ increases linearly, there is a plateau in the DMFT solution corresponding to the diffusive transport. In the AM $D(t)$ reaches a maximum at time $t_{\max}$ and then decreases towards zero. $t_{\max}$ increases with the increase of the localization length. The full solution also features a decrease in diffusion which is, however, interrupted at time $t \approx 1/\omega_0$ when $D(t)$ starts to increase again. This corresponds to the small positive values of $C_{jj}(t)$ for $1/\omega_0 \lesssim t \lesssim 2\pi/\omega_0$ [see the inset of Fig. 1(a)]. The increase in $D(t)$ causes the appearance of an additional zero-frequency peak in $\mu(\omega)$ [Fig. 1(b)]. The agreement between the QC and quantum QT and HEOM solutions is excellent up to $t \lesssim 2\pi/\omega_0$. For larger times, $D(t)$ reaches a clear plateau in QC, while there is a further slight increase in the QT and HEOM solutions. We cannot say if this is due to the finite size of the lattice in a quantum solution ($N = 7$ in QT and $N = 10$ in HEOM). We note that the QC solution is here obtained on the lattice with $N = 200$ sites after averaging over 3000 initial ion displacements and velocities. The backaction term within the Ehrenfest approach leads to very small differences and we show just the CPA results in the main text. For details of the QC numerics, see SM Sec. II [33].

We now discuss a few conceptual issues. First, we note that for the appearance of both the maximum and the minimum in $D(t)$ we need well-separated timescales, $t_{\max}$ being smaller than $1/\omega_0$. $t_{\max}$ is proportional to the localization length L_{loc} in the static case [$L_{\text{loc}}(E_n) = 1/\sum_i |\psi_n^i|^4$, where ψ_n^i are the components of $|\psi_n(0)\rangle$] and at $t \sim 1/\omega_0$ the inelastic electron-phonon scattering comes into effect. The localization length [Fig. 1(d)] depends on the eigenstate energy E_n, while the states near the lower band edge participate in charge transport at low and intermediate temperatures. The notion of these two timescales forms the basis of a popular transient localization scenario of charge transport introduced by Ciuchi, Fratini, and Mayou [4,13]. Yet, the phenomenological TL approach cannot explain the upturn in $\mu(\omega)$ for $\omega < \omega_0$. Within TL, the correlation function $C_{jj}^{\text{TL}}(t) = C_{jj}^{\text{AM}}(t)e^{-t/\tau_{\text{in}}}$ exponentially goes to zero, and $D(t)$ just goes to a constant for $t \gtrsim 1/\omega_0$. We note that the increase of the ensemble-averaged electron kinetic energy $\langle E_{\text{el}}(t) \rangle$ [Fig. 1(e)], which is a well-known artifact of QC dynamics [4], does not significantly influence $C_{jj}^{\text{QC}}(t)$ since the timescale of this increase is significantly longer than the time it takes for C_{jj} to decay to zero. This is in agreement with the findings from a very recent QC study on the Peierls model [21]. Finally, by taking the correlation functions from Fig. 1 as an example, in SM Sec. II [33] we demonstrate why it is impossible to reliably extract the dc mobility just from the imaginary-axis data, which one could obtain from the QMC calculations.

Next, we examine the influence of the temperature to charge transport in Fig. 2. We set a weaker electron-phonon coupling $\lambda = 1/8$ ($g = 0.288$) and consider $T = 5$ (left column) and 0.5 (right column). At high temperature [Figs. 2(a_1)–2(c_1)], the localization length is small [the inset of Fig. 2(c_2)], and the charge dynamics is qualitatively the same as in Fig. 1: Apart from the DDP at finite frequency, there is an additional zero-frequency peak in $\mu(\omega)$. The QC solution (for $N = 100$) agrees very well with the quantum (HEOM) solution (for $N = 7$) [11,24]. At lower temperature [Figs. 2(a_2)–2(c_2)], one needs a longer chain to eliminate the finite-size effects and the HEOM or QT solution are not available. Yet, for a comparison we can use the DMFT

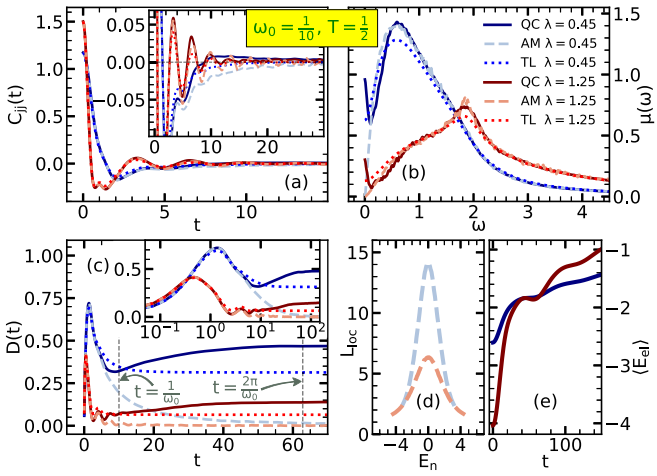

FIG. 3. The same quantities as in Fig. 1 for lower phonon frequency and for an intermediate and strong electron-phonon coupling.

solution, which is in the thermodynamic limit, since we know that the importance of vertex corrections decreases for weaker electron-phonon interactions and lower temperature [11]. DMFT and QC results are in excellent agreement. This is favored by a slower increase of $\langle E_{\rm el}(t)\rangle$ in the weak-coupling case (see SM Sec. II [33]). The dynamical disorder is small at $T = 0.5$, which corresponds to a large localization length and $t_{\rm max}$. Since $t_{\rm max} > 1/\omega_0$, here we do not observe the TL phenomenology.

The electron dynamics for a lower phonon frequency $\omega_0 = 0.1$ is presented in Fig. 3. Here, we do not have a fully quantum solution since one would need a large lattice size and propagation of the correlation function up to very long times. Yet, the previous analysis gives us confidence that the QC approach gives a proper description of the electron dynamics also for a lower phonon frequency. The results at $T = 0.5$ for $\lambda = 0.45$ ($g = 0.3$) and $\lambda = 1.25$ ($g = 0.5$) look qualitatively the same as in Fig. 1. Most importantly, in the time interval $1/\omega_0 \lesssim t \lesssim 2\pi/\omega_0$ the correlation function assumes small positive values [Fig. 3(a)], which leads to the upturn in $\mu(\omega)$ for $\omega < \omega_0$ [Fig. 3(b)]. The diffusion constant $D(t)$ reaches a plateau at $t \sim 2\pi/\omega_0$, as before [Fig. 3(c)]. The displaced peak in $\mu(\omega)$ is centered at a lower frequency for $\lambda = 0.45$ than for $\lambda = 1.25$ when in the AM the localization length is longer [Fig. 3(d)]. We expect that the QC solution is quantitatively better for weaker electron-phonon coupling, when the increase in the electron kinetic energy in the QC solution is not substantial by the time that the plateau in $D(t)$ is reached [Fig. 3(e)]. The TL solution, which does not feature the upturn at long times (low frequency), is shown for comparison.

Conclusions. In summary, we performed QC calculations of charge transport in the 1D Holstein model for two representative phonon frequencies. Frequency $\omega_0 = 0.1$ for temperature $T = 0.5$ is appropriate for the modeling of organic semiconductors such as rubrene, and the results for $\omega_0 = 1/3$ and various g and T are used for a comparison with fully quantum HEOM [24,25] and QT solutions [23]. The agreement between these two quantum methods is excellent. Both methods can propagate the real-time correlation function up to long times and for lattice sizes which are representative of the thermodynamic limit. These properties gave us an opportunity to make detailed comparisons with the QC dynamics, which is performed on much longer chains, consisting of a few hundred lattice sites. For temperatures $T \gtrsim \omega_0$, we find that the charge dynamics is qualitatively the same, and quantitatively quite similar to the quantum case. For strong dynamical disorder, we observe a nonmonotonic diffusion $D(t)$. The maximum in $D(t)$ at short times corresponds to the displaced Drude peak in $\mu(\omega)$ as a precursor to the Anderson localization. At times $1/\omega_0 \lesssim t \lesssim 2\pi/\omega_0$, diffusion increases before reaching a plateau at $t \sim 2\pi/\omega_0$. This corresponds to the upturn in $\mu(\omega)$ for $\omega < \omega_0$. This feature appears regardless of the specific methodology that we used, which gives us confidence that it is a genuine property of the model. The zero-frequency peak in $\mu(\omega)$ does not appear in the TL model of charge transport [4] which, therefore, underestimates the dc mobility. Such a peak is also observed in very recent QC calculations in the Peierls model [21]. This indicates that the peak appears both for local and nonlocal electron-phonon coupling. Our work overcomes the constraints of a small lattice size in real-frequency Lanczos calculations or the analytical continuation of the imaginary-frequency data [12] and presents an explicit comparison between the charge transport in models featuring quantum and classical phonons.

Acknowledgments. We thank V. Janković for fruitful discussions. D.T. thanks J. Mravlje for useful discussions. P.M. and D.T. acknowledge funding provided by the Institute of Physics Belgrade through a grant from the Ministry of Science, Technological Development, and Innovation of the Republic of Serbia. Work in Florida (V.D.) was supported by the NSF Grant No. DMR-2409911, and the National High Magnetic Field Laboratory through the NSF Cooperative Agreement No. DMR-2128556 and the State of Florida.

Data availability. The data that support the findings of this article are openly available [40].

[1] V. Coropceanu, J. Cornil, D. A. da Silva Filho, Y. Olivier, R. Silbey, and J.-L. Brédas, Charge transport in organic semiconductors, Chem. Rev. **107**, 926 (2007).

[2] A. Zhugayevych and S. Tretiak, Theoretical description of structural and electronic properties of organic photovoltaic materials, Annu. Rev. Phys. Chem. **66**, 305 (2015).

[3] S. Fratini, M. Nikolka, A. Salleo, G. Schweicher, and H. Sirringhaus, Charge transport in high-mobility conjugated polymers and molecular semiconductors, Nat. Mater. **19**, 491 (2020).

[4] S. Fratini, D. Mayou, and S. Ciuchi, The transient localization scenario for charge transport in crystalline organic materials, Adv. Funct. Mater. **26**, 2292 (2016).

[5] A. Troisi, Charge transport in high mobility molecular semiconductors: Classical models and new theories, Chem. Soc. Rev. **40**, 2347 (2011).

[6] G. Schubert, G. Wellein, A. Weisse, A. Alvermann, and H. Fehske, Optical absorption and activated transport in polaronic systems, Phys. Rev. B **72**, 104304 (2005).
[7] H. Rammal, A. Ralko, S. Ciuchi, and S. Fratini, Transient localization from the interaction with quantum bosons, Phys. Rev. Lett. **132**, 266502 (2024).
[8] A. S. Mishchenko, N. Nagaosa, G. De Filippis, A. de Candia, and V. Cataudella, Mobility of Holstein polaron at finite temperature: An unbiased approach, Phys. Rev. Lett. **114**, 146401 (2015).
[9] H. B. Meyer, Transport properties of the quark-gluon plasma: A lattice QCD perspective, Eur. Phys. J. A **47**, 86 (2011).
[10] J. Vučičević, J. Kokalj, R. Žitko, N. Wentzell, D. Tanasković, and J. Mravlje, Conductivity in the square lattice Hubbard model at high temperatures: Importance of vertex corrections, Phys. Rev. Lett. **123**, 036601 (2019).
[11] V. Janković, P. Mitrić, D. Tanasković, and N. Vukmirović, Vertex corrections to conductivity in the Holstein model: A numerical-analytical study, Phys. Rev. B **109**, 214312 (2024).
[12] P. Buividovich, J. Ostmeyer, and A. Troisi, High-precision Quantum Monte-Carlo study of charge transport in a lattice model of molecular organic semiconductors, PoS **(LATTICE2024)**, 067 (2024).
[13] S. Ciuchi, S. Fratini, and D. Mayou, Transient localization in crystalline organic semiconductors, Phys. Rev. B **83**, 081202(R) (2011).
[14] A. Pustogow, Y. Saito, A. Löhle, M. Sanz Alonso, A. Kawamoto, V. Dobrosavljević, M. Dressel, and S. Fratini, Rise and fall of Landau's quasiparticles while approaching the Mott transition, Nat. Commun. **12**, 1571 (2021).
[15] S. Fratini and S. Ciuchi, Displaced Drude peak and bad metal from the interaction with slow fluctuations, SciPost Phys. **11**, 039 (2021).
[16] J. Keski-Rahkonen, X. Ouyang, S. Yuan, A. M. Graf, A. Aydin, and E. J. Heller, Quantum-acoustical Drude peak shift, Phys. Rev. Lett. **132**, 186303 (2024).
[17] A. Aydin, J. Keski-Rahkonen, and E. J. Heller, Quantum acoustics unravels Planckian resistivity, Proc. Natl. Acad. Sci. USA **121**, e2404853121 (2024).
[18] J. C. Tully, Ehrenfest dynamics with quantum mechanical nuclei, Chem. Phys. Lett. **816**, 140396 (2023).
[19] A. Troisi and G. Orlandi, Charge-transport regime of crystalline organic semiconductors: Diffusion limited by thermal off-diagonal electronic disorder, Phys. Rev. Lett. **96**, 086601 (2006).
[20] J. H. Fetherolf, D. Golež, and T. C. Berkelbach, A unification of the Holstein polaron and dynamic disorder pictures of charge transport in organic crystals, Phys. Rev. X **10**, 021062 (2020).
[21] J. E. Runeson, T. J. G. Drayton, and D. E. Manolopoulos, Charge transport in organic semiconductors from the mapping approach to surface hopping, J. Chem. Phys. **161**, 144102 (2024).
[22] J. E. Runeson and D. E. Manolopoulos, A multi-state mapping approach to surface hopping, J. Chem. Phys. **159**, 094115 (2023).
[23] P. Mitrić, Dynamical quantum typicality: A simple method for investigating transport properties applied to the Holstein model, arXiv:2412.17436.
[24] V. Janković, Holstein polaron transport from numerically "exact" real-time quantum dynamics simulations, J. Chem. Phys. **159**, 094113 (2023).
[25] V. Janković, Numerical study of the one-dimensional Holstein model using the momentum-space hierarchical equations of motion method, Zenodo, https://zenodo.org/records/8068547.
[26] R. Kubo, Statistical-mechanical theory of irreversible processes. I. General theory and simple applications to magnetic and conduction problems, J. Phys. Soc. Jpn. **12**, 570 (1957).
[27] G. Mahan, *Many-Particle Physics* (Plenum, New York, 1990).
[28] B. Bertini, F. Heidrich-Meisner, C. Karrasch, T. Prosen, R. Steinigeweg, and M. Žnidarič, Finite-temperature transport in one-dimensional quantum lattice models, Rev. Mod. Phys. **93**, 025003 (2021).
[29] T. Heitmann, J. Richter, D. Schubert, and R. Steinigeweg, Selected applications of typicality to real-time dynamics of quantum many-body systems, Z. Naturforsch. A **75**, 421 (2020).
[30] F. Jin, D. Willsch, M. Willsch, H. Lagemann, K. Michielsen, and H. De Raedt, Random state technology, J. Phys. Soc. Jpn. **90**, 012001 (2021).
[31] S. Ciuchi, F. de Pasquale, S. Fratini, and D. Feinberg, Dynamical mean-field theory of the small polaron, Phys. Rev. B **56**, 4494 (1997).
[32] P. Mitrić, V. Janković, N. Vukmirović, and D. Tanasković, Spectral functions of the Holstein polaron: Exact and approximate solutions, Phys. Rev. Lett. **129**, 096401 (2022).
[33] See Supplemental Material at http://link.aps.org/supplemental/10.1103/PhysRevB.111.L161105 for analytical derivations and additional numerical results.
[34] C. Cohen-Tannoudji, B. Diu, and F. Laloë, *Quantum Mechanics*, 1st ed. (Wiley, New York, 1977).
[35] W. Greiner, *Quantum Mechanics: An Introduction*, 3rd ed. (Springer, Berlin, 1994).
[36] L. Landau and E. M. Lifshitz, *Quantum Mechanics (Non-Relativistic Theory)*, 3rd ed. (Elsevier/Butterworth-Heinemann, Oxford, UK, 2013).
[37] R. van Leeuwen and N. E. Dahlen, An introduction to nonequilibrium Green functions, Lecture notes, https://www.theochem.ru.nl/han/2004/NGF.pdf.
[38] H. Aoki, N. Tsuji, M. Eckstein, M. Kollar, T. Oka, and P. Werner, Nonequilibrium dynamical mean-field theory and its applications, Rev. Mod. Phys. **86**, 779 (2014).
[39] L. Wang, D. Beljonne, L. Chen, and Q. Shi, Mixed quantum-classical simulations of charge transport in organic materials: Numerical benchmark of the Su-Schrieffer-Heeger model, J. Chem. Phys. **134**, 244116 (2011).
[40] P. Mitrić, V. Dobrosavljević, and D. Tanasković, Data for "Precursors to Anderson localization in the Holstein model: Quantum and quantum-classical solutions", Zenodo, https://doi.org/10.5281/zenodo.15011362.

Correction: A grant number in the Acknowledgments contained an error and has been fixed.